

- [13] M. Zhang, E. Ciocan, Y. Bando, K. Wada, L. L. Cheng, P. Pirouz, *Appl. Phys. Lett.* **2002**, *80*, 491.
- [14] R. Fan, Y. Wu, D. Li, M. Yue, A. Majumdar, P. Yang, *J. Am. Chem. Soc.* **2003**, *125*, 5254.
- [15] Y. B. Li, Y. Bando, D. Golberg, Y. Uemura, *Appl. Phys. Lett.* **2003**, *83*, 3999.
- [16] S. O. Obare, N. R. Jana, C. J. Murphy, *Nano Lett.* **2001**, *1*, 601.
- [17] Y. D. Yin, Y. Lu, Y. G. Sun, Y. N. Xia, *Nano Lett.* **2002**, *2*, 427.
- [18] W. Shenton, T. Douglas, M. Young, G. Stubbs, S. Mann, *Adv. Mater.* **1999**, *11*, 253.
- [19] Y. Ono, Y. Kanekiyo, K. Inoue, J. Hojo, M. Nango, S. Shinkai, *Chem. Lett.* **1999**, 475.
- [20] a) L. Wang, S. Tomura, F. Ohashi, M. Maeda, M. Suzuka, K. Inukai, *J. Mater. Chem.* **2001**, *11*, 1456. b) F. Miyai, S. A. Davis, J. P. H. Charmant, S. Mann, *Chem. Mater.* **1999**, *11*, 3021.
- [21] S. Mann, S. Burkett, S. A. Davis, C. Fowler, N. H. Mendelson, S. D. Sims, D. Walsh, N. Whiton, *Chem. Mater.* **1997**, *9*, 2300.
- [22] a) Y. Ono, K. Nakashima, M. Sano, Y. Kanekiyo, K. Inoue, J. Hojo, S. Shinkai, *Chem. Commun.* **1998**, 1477. b) J. H. Jung, Y. Ono, S. Shinkai, *Angew. Chem. Int. Ed.* **2000**, *39*, 1862. c) J. H. Jung, K. Nakashima, S. Shinkai, *Nano Lett.* **2001**, *1*, 145.
- [23] J. H. Jung, Y. Ono, K. Hanabusa, S. Shinkai, *J. Am. Chem. Soc.* **2000**, *122*, 5008.
- [24] J. H. Jung, M. Amaike, S. Shinkai, *Chem. Commun.* **2000**, 2343.
- [25] J. H. Jung, S. Shinkai, T. Shimizu, *Nano Lett.* **2002**, *2*, 17.
- [26] M. Jansen, K. Heidebrecht, R. Matthes, W. Eysel, *Z. Anorg. Allg. Chem.* **1991**, 601, 5.
- [27] a) S. H. Yu, B. Liu, M. S. Mo, J. H. Huang, X. M. Liu, Y. T. Qian, *Adv. Funct. Mater.* **2003**, *13*, 639. b) X. J. Cui, S. H. Yu, L. L. Li, B. Liu, H. B. Li, M. S. Mo, X. M. Liu, *Chem. Eur. J.* **2003**, *9*, 218.
- [28] a) X. Bao, M. Muhler, T. Schedel-Niedrig, R. Schlögl, *Phys. Rev. B* **1996**, *54*, 2249. b) S. W. Gaarenstroom, N. Winograd, *J. Chem. Phys.* **1977**, *67*, 3500.

High-Performance All-Polymer Transistor Utilizing a Hygroscopic Insulator**

By Henrik G. O. Sandberg,* Tomas G. Bäcklund, Ronald Österbacka, and Henrik Stubb

The performance of organic field-effect transistors, OFETs, restricts their potential use to applications where low efficiency and short lifetimes are acceptable, although recently the field has evolved rapidly.^[1,2] Proposed applications are radio-

frequency information tags, e.g., price tags and inventory labels, sensors, and simple displays.^[3–6] A simple, low-cost manufacturing process is desired, however such processes usually result in significantly lower device performance.

The manufacture of state-of-the-art OFETs today^[7] normally requires the device to be processed in an inert atmosphere and to be shielded from oxygen and humidity in the air.^[8] The best organic transistors have almost reached the performance levels of amorphous silicon devices and the technology is entering the commercial stage.^[9–13]

We report on the manufacture and characteristics of a high-performance OFET. The special feature of the device is its ability to take advantage of ambient moisture by using a hygroscopic gate dielectric. (The device is hereafter referred to as hygroscopic insulator field-effect transistor, HIFET.) The all-polymer HIFET can be produced by a solution process using printing techniques onto flexible plastic substrates where all processing steps can be performed without requiring controlled atmosphere. We record a one-hundred-fold enhancement in measured currents at low drive voltages of only a few volts, with good current saturation and current modulation in ambient atmosphere. The static performance of the device characterized by current level and modulation at low voltages (less than 1 V) is greatly enhanced by moisture in the hygroscopic insulator. This study concentrates on the novel device characteristics and proposes an explanation for the device operation mechanism.

The HIFET measured in room atmosphere shows excellent performance in terms of current level and modulation, as can be seen from the output curve in Figure 1A. The current saturates at less than 1 V on the drain electrode for a low constant

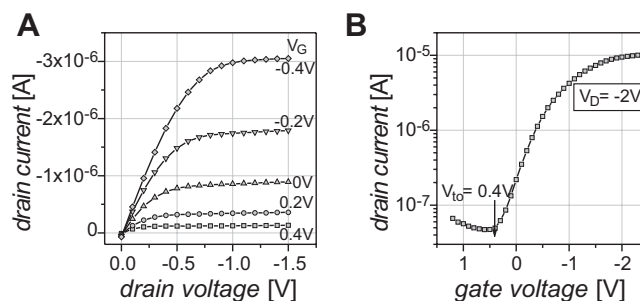


Figure 1. Device characteristics and structure of an all-polymer field-effect transistor, HIFET, measured in ambient air. A) Output curve plotting the drain current as a function of drain voltage at gate voltages ranging from 0.4 V to -0.4 V. The device is built on prepatterned polyaniline source–drain electrodes with a channel of length $L=20$ μm and width $W=7.2$ mm. B) The transfer curve of the same sample showing a turn-on voltage of 0.4 V.

gate voltage (V_G varied within less than ± 1 V), indicating a threshold voltage close to 0 V. The corresponding transfer curve in the saturated region is shown in Figure 1B, from which the turn on voltage (V_{to}) and the ON/OFF ratio can be estimated to be 0.4 V and ~ 200 , respectively. Here, V_{to} is given

[*] Dr. H. G. O. Sandberg,^[†] T. G. Bäcklund, Dr. R. Österbacka, Prof. H. Stubb
Department of Physics, Åbo Akademi University
Porthansgatan 3, 20500 ÅBO (Finland)
E-mail: henrik.sandberg@abo.fi

[†] Second address: Graduate School of Materials Research, Turku University and Åbo Akademi University, Porthansgatan 3, 20500 ÅBO, Finland.

[**] We thank T. Mäkelä and S. Jussila for help with electrode fabrication. Financial support through the Finnish Technology Development Centre (Tekes) project MUOELE, and the Academy of Finland grant no 50575.

en instead of the threshold voltage, V_T , because of the large OFF current. The sub-threshold swing, S , can be estimated to be ~ 0.5 V decade $^{-1}$. Similar traditional devices have $V_T > 10$ – 20 V, requiring extensive sample and substrate conditioning to reduce V_T .^[14] To demonstrate long-term stability the same all-polymer HIFET was tested after more than one year of storage in normal room conditions and showed nearly identical current modulation behavior, despite a current level decrease by 1–2 decades, which could be caused by, e.g., relative humidity variations. There are indications, however, that repeated extreme humidity variations degrade device performance.

There have been reports of the same materials^[15] and of similar devices showing gas sensitivity^[16] and electrochemical action,^[17,18] but none presenting the features of the HIFET. Figures 2A,B show a HIFET output and transfer curve, respectively, measured in humid air (relative humidity, RH, ~ 35 %). The same HIFET measured in pure dry nitrogen is shown in Figure 2D where the saturation and modulation behavior is absent, while in Figure 2C (anhydrous) methanol fumes are added to the measurement chamber, restoring the current modulation. Notably the HIFET shows good performance with solvent fumes of small and polar molecules, while larger and non-polar molecules (solvents like *n*-hexane, *p*-xylene, and tetrahydrofuran were tested) give only straight-line current–voltage curves reflecting the conductivity of the semiconductor material, as do devices measured in dry-nitrogen conditions (Fig. 2D) or dry air. In the latter case the device

functions as a traditional OFET with a high doping level of the semiconductor. For such samples only the linear region of the current–voltage curve is probed, even when using voltages of tens of volts. If polystyrene or poly(methyl methacrylate) is used as gate-insulator material the device does not show HIFET behavior. The all-polymer HIFET device performance is maintained even when the sample is bent as shown in Figure 2E. Figure 2F shows the drain current in the saturated region over time as the gate voltage is switched. Characteristic of the device is a settling time for the current of some seconds as the gate field is shifted displaying the limited dynamic switching properties of the device. These transistors can be used in, e.g., amplifier circuits only for low-frequency applications. Since all the transistor current–voltage curves above are measured at low scan speeds (0.1 V s $^{-1}$) the unique device characteristics are not affected by the settling time of the current. The transfer curve is more sensitive to the settling time of the gate modulation. Thus, the hysteresis seen in Figure 2B depends on the scan rate and arises from the ion-modulated mode of operation of the device.

As a result of the current-modulation effect, the high currents recorded for the HIFET cannot be attributed solely to a very high conductivity of the sample. Despite the excellent behavior of the output current–voltage curves the ON/OFF ratio is on the order of 10^2 – 10^3 .

Figure 3A shows the mobility versus conductivity for the HIFET and traditional OFET samples, the latter being measured using the higher voltages required for OFETs, under

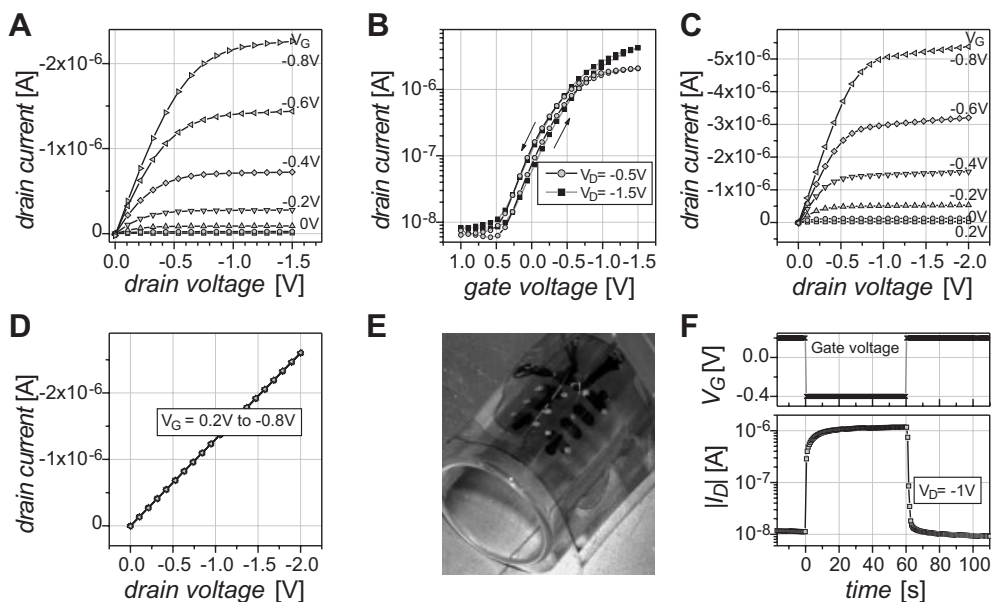


Figure 2. Current–voltage characteristics of the polymer HIFET device under different environmental conditions. A) The output curves of a fresh HIFET with gold source and drain electrodes measured in humid air (RH ~ 35 %). B) The corresponding transfer curve ($V_{D0} = 0.4$ V, same as in Fig. 1B). C) The output curves of a HIFET device measured in an atmosphere of saturated methanol in dry nitrogen. D) The same curves at dry (N_2) conditions. When the sample is removed from humid air (or other atmosphere containing light polar solvent vapor) the typical transistor current–voltage output is lost and only the conductivity of the film is measured. The flexible HIFET can be bent and measured without losing performance. E) The measured sample bent to a radius of ~ 8 mm. Output characteristics are similar to those of the fresh sample shown in (A). F) The response in drain current with a constant drain voltage as a voltage pulse (upper panel) is applied to the gate contact.

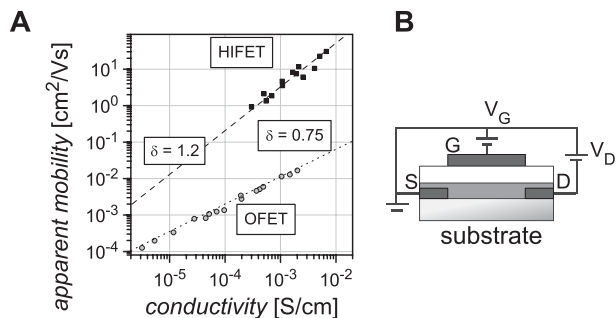


Figure 3. HIFET and traditional OFET μ versus σ behavior. The “apparent mobility” is the field-effect charge carrier mobility as estimated from the current–voltage curves according to common theory [19]. A) Standard OFETs follow a universal relationship between mobility and conductivity (see ref. [20]). Circles show different measurements on both organic and hybrid inorganic-organic OFETs that do not represent the HIFET reported in this paper. The $\delta = 0.75$ value follows the “universal rule” of Equation 1 (dotted line). Squares show the apparent mobility versus conductivity of HIFET devices. B) The schematic device and measurement setup. G, S, and D refer to the transistor electrodes gate, source and drain, respectively.

dry conditions using regioregular poly(3-hexylthiophene) (RR-P3HT) as the semiconductor material and polyvinylphenol (PVP) as an insulator material. The mobility values were estimated using the standard equations^[19] for thin-film transistors (TFTs) in both the saturated and the linear region, and were used in the case of the HIFET to provide comparison with commonly presented results. All points representing traditional OFETs follow a line marked by the “universal rule”^[20]

$$\mu_{FE} \approx \sigma^\delta \quad (1)$$

with $\delta \approx 0.7$ which holds for a large range of amorphous materials and samples where μ_{FE} is the field-effect mobility and σ is the conductivity of the sample. The HIFET samples do not, however, follow this rule but have a steeper slope (larger δ ; marked by the dashed line in Fig. 3A) and a shift to mobility values about 100 times larger, despite containing the same semiconducting material. This indicates a different transport environment in the FET channel region. We note that the apparent mobility value estimated using standard theory,^[19] of the order of $100 \text{ cm}^2 \text{ V}^{-1} \text{ s}^{-1}$ for this device, is not physical if considered as a traditional field effect. The apparent mobility of the HIFET should be considered a number to quantify the performance of the device as it comes to current magnitude and modulation at a certain voltage, even though the performance relies on the mechanisms proposed below and not a pure field effect. Other characteristics for the HIFET, e.g., the switching speed and amplitude and the gate current (often on the order of nA for working HIFETs), have to be accounted for by new mechanisms. The apparent mobility is a “device mobility” incorporating the field-effect and the humidity-induced effects, pure RR-P3HT charge carrier mobility is reflected by the dotted line in Figure 3A.

We propose a mechanism where the gate field modulation of the drain current is enhanced by an ionic process that occurs in the moisturized gate dielectric close to the semiconductor interface. The mechanism involves movement of ionic species within the moisturized insulator layer of the device structure assisting the pinch-off effect and the increased conductivity through modulation of charge carrier concentration in the transistor channel region. Samples using gold gate electrodes show the same effect indicating that the field-effect mechanism does not rely on the water-soluble poly(3,4-ethylenedioxythiophene):poly(styrene sulfonate) PEDOT:PSS material. However, gold acts as a diffusion barrier for humidity into the insulator, increasing the time of response to humidity changes.

The ionic drift is very sensitive to the gate field giving a turn on voltage, V_{to} , very close to 0 V. The current enhancement is a sum of two possible mechanisms that are hard to separate experimentally: i) drift of mobile ions (e.g., H^+ , Na^+ , Cl^- , OH^- , ...) in the PVP layer giving pinch-off at the drain contact and drain current modulation by shifting electric charge close to the semiconductor interface, ii) direct electrochemical doping of the semiconductor ($\text{P3HT} + \text{A}^+\text{C}^- \leftrightarrow \text{P3HT}^+\text{C}^- + \text{A}^+ + \text{e}^-$, where A^+ is an anionic and C^- a cationic impurity) and the diffusion of ionic impurities through the PVP–RR-P3HT interface. The hygroscopic insulator and the presence of a solvent are essential for the operation of the HIFET which is shown by the loss of current modulation when drying out the insulator. Exposing the semiconductor layer of a traditional OFET structure to moisture does not result in HIFET behavior. RR-P3HT is probably the most suitable active material, since the charge carriers can easily delocalize due to the large intermolecular coupling between the individual chains.^[13,21] We have not been able to identify the source of the ions (PVP or RR-P3HT materials) that are most probably residual contaminants from the synthesis. With moisture absorbed in the PVP layer, ions are mobile enhancing device performance. Mobile negative ions in PVP moving into the PVP–RR-P3HT interface may cause electrochemical doping of the semiconductor at the interface. On the other hand, positive ions in the PVP–RR-P3HT interface may get mobile in PVP (attracted by the negative gate potential) and separated from their negative counter-ions resulting in an excess of negative charged species in the vicinity of the RR-P3HT film.

It is well known that insulator material properties influence FET characteristics.^[11,22] Reports on novel devices using highly conducting polymers,^[17,23] however, only probe the metal–insulator transition of a highly doped film. The HIFET, on the other hand, works in accumulation mode where the current is increased by a larger gate field, in accordance with normal TFT behavior. Reported electrochemical FETs differ from the present structure as they have a gate dielectric entirely replaced by an electrolyte,^[24] e.g., a filterpaper wetted with an acid.^[25]

We have presented a hygroscopic insulator field-effect transistor with a performance, when operated in air, greatly supe-

rior to traditional organic devices in terms of current modulation at low voltages and turn-on voltage close to 0 V. The device is compatible with large-area low-cost fabrication procedures, i.e., printing techniques, and does not require any fabrication steps in controlled atmosphere. Device characteristics have been shown and an explanation for the behavior has been suggested.

Experimental

Transistors were prepared using as the active semiconductor material regioregular poly(3-hexylthiophene), RR-P3HT, from different suppliers such as American Dye Source, Merck Inc., and Aldrich. RR-P3HT was spin-coated from solution in *p*-xylene or chloroform (concentration 4–10 mg mL⁻¹) at a speed of 1000–1500 rpm for 30 s and dried on a hotplate (70 °C) for 10 min. As a gate-dielectric material for the HIFET polyvinylphenol, PVP, from Aldrich ($M_w \sim 20\,000$) or ChemFirst/DuPont (called polyhydroxystyrene; $M_w \sim 25\,000$) was spin-coated (1500 rpm, 30 s) from solution in ethyl acetate (100 mg mL⁻¹) and dried on a hotplate (70 °C, 20 min) giving a film thickness of $\sim 1\ \mu\text{m}$. All materials were used as received and there was no considerable difference in device performance between samples made from different sources, despite variations, e.g., in terms of material purity.

The gate electrode was prepared from poly(3,4-ethylenedioxythiophene) poly(styrene sulfonate), PEDOT:PSS, purchased from H. C. Starck GmbH as “Baytron P” and used as received. As substrates poly(ethylene terephthalate) (PET) films from Teijin Films were used. Where pre-patterned substrates were used source and drain electrodes, interdigitated finger structures were prepared by photolithographic methods from conducting polyaniline, PANI (in a toluene solution from Panipol Oy). Gold source and drain electrodes were prepared by thermal evaporation through a shadow mask under vacuum, defining channel areas 1500 μm wide and 35 or 100 μm long. As it was found that the electrode material does not influence this novel device behavior, metal source and drain electrodes were used for simplicity. The gate electrode was prepared by depositing a droplet of PEDOT:PSS solution of a size that covers the transistor channel region. The PEDOT:PSS was left to dry in air at room temperature. All materials used here have been previously used in organic FETs but without addressing this phenomenon. PVP is normally used with a crosslinking substance [3,26] which should change the hygroscopic properties of the gate insulator.

The reference “traditional” OFET was prepared using an extensively cleaned Si/SiO₂ (300 nm oxide thickness) substrate, onto which a thin layer of RR-P3HT was deposited by spin-coating from solution. Gold source and drain electrodes were evaporated in vacuum through a shadow mask to define the transistor channel area, typically of length $L = 35\ \mu\text{m}$ and width $W = 1500\ \mu\text{m}$. The rigid highly doped substrate of the FET was used as the gate. The reference transistor was prepared and measured in controlled dry N₂ atmosphere to avoid unintentional doping of the exposed semiconductor film. Before measurement the sample was vacuum-annealed overnight at 100 °C. All device characteristics were measured using an Agilent 4142B parameter analyzer controlled by a computer. The scan rate for the current–voltage curves was 0.1 V s⁻¹. The capacitance of the PVP layer was measured using several techniques to be 4.3 nF cm⁻² for a dry sample. Under ambient atmosphere the capacitance increases with 20–40 % depending on for example the relative humidity level and the time of exposure.

Received: January 9, 2004

Final version: February 27, 2004

- [1] J. Rogers, Z. Bao, *J. Polym. Sci., Part A: Polym. Chem.* **2002**, *40*, 3327.
- [2] V. Saxena, B. D. Malhotra, *Curr. Appl. Phys.* **2003**, *3*, 293.
- [3] C. J. Drury, C. M. J. Mutsaers, C. M. Hart, M. Matters, D. M. de Leeuw, *Appl. Phys. Lett.* **1998**, *73*, 108.
- [4] H. E. A. Huitema, G. H. Gelinck, J. B. P. H. van der Putten, K. E. Kuijk, C. M. Hart, E. Cantatore, P. T. Herwig, A. J. M. M. van Breemen, D. M. de Leeuw, *Nature* **2001**, *414*, 599.
- [5] P. Mach, S. J. Rodriguez, R. Nortrup, P. Wiltzius, J. A. Rogers, *Appl. Phys. Lett.* **2001**, *78*, 3592.
- [6] C. D. Sheraw, L. Zhou, J. R. Huang, D. J. Gundlach, T. N. Jackson, M. G. Kane, I. G. Hill, M. S. Hammond, J. Campi, B. K. Greening, J. Francl, J. West, *Appl. Phys. Lett.* **2002**, *80*, 1088.
- [7] H. Sirringhaus, T. Kawase, R. H. Friend, *US Patent Application Publication US2003/0059984 A1*, **2003**.
- [8] B.-H. Huisman, J. Valetton, W. Nijssen, J. Lub, W. ten Hoeve, *Adv. Mater.* **2003**, *15*, 2002.
- [9] K. R. Amundson, B. J. Sapjeta, A. J. Lovinger, Z. N. Bao, *Thin Solid Films* **2002**, *414*, 143.
- [10] X. Chen, Z. Bao, H. Schon, A. Lovinger, Y. Lin, B. Crone, A. Doda-balapur, B. Batlogg, *Appl. Phys. Lett.* **2001**, *78*, 228.
- [11] M. Halik, K. Hagen, U. Zschieschang, G. Schmidt, W. Radlik, W. Weber, *Adv. Mater.* **2002**, *14*, 1717.
- [12] S. K. Park, Y. H. Kim, J. I. Han, D. G. Moon, W. K. Kim, *IEEE Trans. Electron Devices* **2002**, *49*, 2008.
- [13] H. Sirringhaus, P. J. Brown, R. H. Friend, M. M. Nielsen, K. Bechgaard, B. M. W. Langeveld-Voss, A. J. H. Spiering, R. A. J. Janssen, E. W. Meijer, P. Herwig, D. M. de Leeuw, *Nature* **1999**, *401*, 685.
- [14] E. J. Meijer, C. Detcheverry, P. J. Baesjou, E. van Veenendaal, D. M. de Leeuw, T. M. Klapwijk, *J. Appl. Phys.* **2003**, *93*, 4831.
- [15] H. Sirringhaus, N. Tessler, R. H. Friend, *Science* **1998**, *280*, 1741.
- [16] Y. Ohmori, H. Takahashi, K. Muro, M. Uchida, T. Kawai, K. Yoshino, *Jpn. J. Appl. Phys., Part 2* **1991**, *30*, L1247.
- [17] A. J. Epstein, F.-C. Hsu, N.-R. Chiou, V. N. Prigodin, *Curr. Appl. Phys.* **2002**, *2*, 339.
- [18] D. Nilsson, M. X. Chen, T. Kugler, T. Remonen, M. Armgarth, M. Berggren, *Adv. Mater.* **2002**, *14*, 51.
- [19] S. M. Sze, *Physics of Semiconductor Devices*, Wiley, New York **1981**.
- [20] A. Brown, C. Jarrett, D. de Leeuw, M. Matters, *Synth. Met.* **1997**, *88*, 37.
- [21] R. Österbacka, C. P. An, X. M. Jiang, Z. V. Vardeny, *Science* **2000**, *287*, 839.
- [22] J. Veres, S. D. Ogier, S. W. Leeming, D. C. Cupertino, S. M. Khaffaf, *Adv. Funct. Mater.* **2003**, *13*, 199.
- [23] A. J. Epstein, F.-C. Hsu, N.-R. Chiou, V. N. Prigodin, *Synth. Met.* **2003**, *137*, 859.
- [24] S. Chao, M. Wrighton, *J. Am. Chem. Soc.* **1987**, *109*, 6627.
- [25] V. Rani, K. S. V. Santhanam, *J. Solid State Electrochem.* **1998**, *2*, 99.
- [26] U. Zschieschang, H. Klauk, M. Halik, G. Schmid, C. Dehm, *Adv. Mater.* **2003**, *15*, 1147.